Journal of Sound and Vibration 326 (2009) 809–820

Contents lists available at ScienceDirect

Journal of Sound and Vibration

journal homepage: www.elsevier.com/locate/jsvi

Chip formation as an oscillator during the turning process

Zoltán Pálmai [a], Gábor Csernák [b,*]

[a] COGITO Ltd., Alvinci u. 24., H-1022 Budapest, Hungary
[b] HAS-BUTE Research Group on Dynamics of Machines and Vehicles, H-1521 Budapest, Hungary

ARTICLE INFO

Article history:
Received 1 October 2008
Received in revised form
2 April 2009
Accepted 22 May 2009
Handling Editor: M.P. Cartmell
Available online 17 June 2009

ABSTRACT

Previously we put forward a thermomechanical model for the description of the process of chip formation. Now, this model is supplemented with the differential equation of the oscillating workpiece. The chip formation may provide an excitation within the machine-tool-workpiece system. Taking this interaction into consideration is expedient during the design of the machining technology, in order to avoid harmful vibrations. From this point of view, the chip formation can be considered as an oscillator. We analyse the expanded model and point out that the vibrations of the workpiece may lead to rather complex motions.

1. Introduction

Oscillations of cutting machine-tool-workpiece systems have occupied the attention of theoreticians and technologists for more than 80 years. Armarego and Brown [2] compiled a thorough overview of the topic in 1969, based on Tobias' fundamental work [1] and that of several other researchers. Tlusty [3] collected even more references. This topic is still a high priority in machine production research.

Doi [4] perceived the importance of self-induced vibrations during cutting as early as in 1937. The three forms of this phenomenon are as follows:

(a) The *built-up-edge* was first examined in detail by Ernst and Martellotti [5], who pointed out that the edge continuously builds up and tears off, generating periodic variations in the cutting force. The frequency of the evolving oscillations is 77–200 Hz, as shown by Shteinberg [6] 60 years ago.
(b) *Chip segmentation* (Fig. 1) was described first by Piispanen [7]. Landberg [8] examined the phenomenon experimentally, but the detailed analysis was carried out by Albrecht [9]. It is worth highlighting the contribution of Komanduri et al. [10], too. The overview [11] compiled by Komanduri is also interesting because of the published pictures taken of typical chips. The frequency of the excitation due to this phenomenon was in the range 200–4000 Hz.
(c) *Discontinuous-chip formation* was analysed in detail by Field and Merchant [12]. Other interesting contributions to this field are Recht's [13] highly cited paper and Shaw's manuscript about machinability [14]. This chip type can be considered as a limiting case of chip segmentation. Thus, Albrecht's estimation [9] of the frequency range can be applied, leading to $10^3 - 1.5 \times 10^4$ Hz. This approach was verified by Komanduri in several papers (e.g. [15]), who traced back the chip formation process to the characteristics of the material of the workpiece.

* Corresponding author. Tel.: +36 1 463 1227; fax: +36 1 463 3471.
E-mail addresses: palmayz@t-online.hu (Z. Pálmai), csernak@mm.bme.hu (G. Csernák).

0022-460X/$ - see front matter © 2009 Elsevier Ltd. All rights reserved.
doi:10.1016/j.jsv.2009.05.028

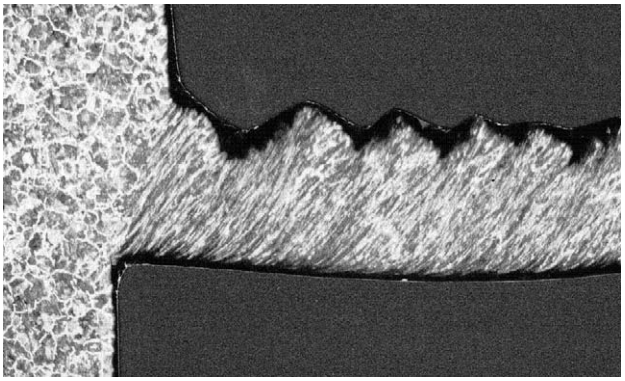

Fig. 1. Formation of segmental chip.

The aforementioned phenomena are all closely related to the material of the workpiece. Besides these cases, the elasticity of the machine-tool-workpiece system may also lead to vibrations.

In the case of regenerative chatter, the undeformed chip thickness cut at time t is influenced by the real chip thickness one revolution earlier, i.e., at $t - T$, where T is the period of rotation. The variation of the chip thickness is the consequence of the oscillations of the tool and the workpiece. Shi and Tobias [16] even took into account the multiple regenerative effect, i.e., that the instantaneous chip thickness may depend on the displacement of the tool at instants $t - T$, $t - 2T$, etc., too. Stépán [17] described the nonlinear regenerative chatter of machine tools with a delayed differential equation. His results were verified experimentally in the case of thread cutting [18]. Gradisek et al. estimated the coarse-grained entropy for the detection of the vibrations during turning [19], while in another paper [20], examined the nonlinear, non-regenerative model of the cutting process. Also, a method was introduced for the analysis of the time series obtained from measurements [21]. Johnson [22] examined a model with combined short delays and regenerative delays, based on the cutting model proposed by Doi and Kato [23]. These results make possible the predictive control of cutting [24]. Rusinek et al. [25] analysed the effect of the surface profile of the workpiece on the regenerative vibrations. Kalmár-Nagy and Moon [26] even took into account the displacements of the tool holder in two directions and the torsion of the tool for the theoretical examination of regenerative phenomena during turning.

Besides the theoretical analysis, the measurement of vibrations of the machining system is also a topic of great interest. Minis and Berger [27] developed their measurement system on the assumption that the cutting process is a closed loop-like dynamical system. Since Grabec [28] pointed out in a nonlinear, 2DoF system—omitting the regenerative effect—that chaotic vibrations may occur during cutting, several research groups have performed experiments in this area. Lin and Weng [29] considered a 1DoF model with regenerative effect, and examined the stability of the process, taking into account the dependence of the cutting force on the cutting speed and chip thickness. They also examined a 2DoF model numerically with multiple regenerative effects, and found chaotic dynamics [30].

Among several other contributions, Berger et al. [31] examined the cutting process with delayed differential equations, while Gans [32] analysed Grabec's results. Moon and Abarbanel [33] and Bukkapatman et al. [34] proved experimentally that machine tool vibration can be chaotic. Rusinek et al. [35] examined the amplitude of the evolving—sometimes resonant—vibrations in a 2DoF, non-regenerative model. Berger et al. [36] showed with the help of the false nearest neighbours (FNN) method that the acceleration of the tool tip is chaotic during the cutting of ductile steel. They also found that the chaotic attractor can be embedded in a four-dimensional (4D) space, thus, its dimension is less than four. Recently, Litak [37] and Litak et al. [38] studied the regenerative chatter phenomenon. In the latter paper, nonlinear time series analysis was applied, just as in [39], by Sen et al., where the dynamics of the cutting process was examined according to a 2DoF model. Comparing the Litak model and the classic delay differential equation model, Wang et al. [40] examined the possibility of the elimination of chaos and large amplitude oscillations. They found that this goal is feasible.

The common feature within the aforementioned contributions is that thermal effects are not taken into account. However, these effects have a great influence on the characteristics of the material of the workpiece, and consequently, on the cutting process itself. The continuum mechanical cutting model, introduced by Burns and Davies [41] already takes into account the thermal processes. The calculations were verified both experimentally and numerically, but the vibrations were not examined.

2. Four-dimensional model of chip forming

In the present contribution, we model the chip segmentation and discontinuous-chip formation in the case of non-regenerative chatter. The excitation of these vibrations is related to the variation of the material characteristics of the workpiece at different cutting speeds and varying temperatures.

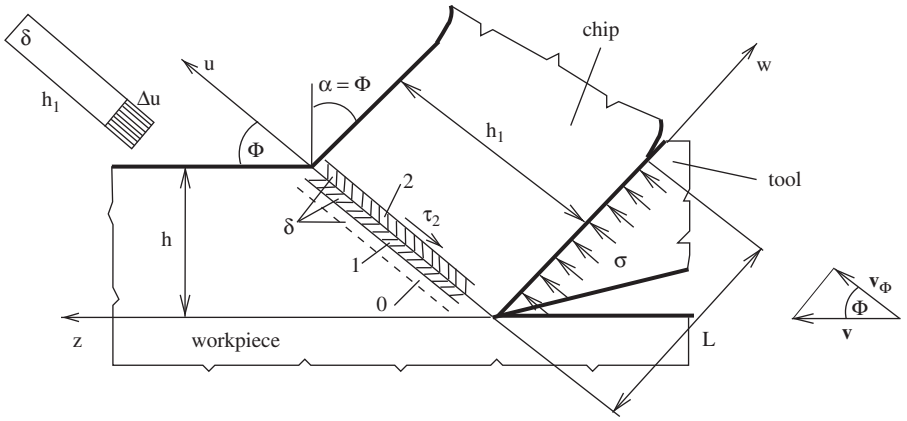

Fig. 2. Simplified model of the shear zone.

During the cutting of metals, the strain-hardening of the material and the thermal softening due to the deformation heat may often lead to thermoplastic instability [15]. The chip forming is either periodic in this case or—under certain circumstances—an aperiodic, chaotic process. The periodic chip formation (Fig. 1) may provide an excitation within the machine-tool-workpiece system. Taking this interaction into consideration is expedient during the design of the machining technology, in order to avoid harmful vibrations. From this point of view, the chip formation can be considered as an oscillator. Previously, a thermomechanical model was put forward for the description of the process of chip formation [42,43], that is based on the simplified technological model, shown in Fig. 2. The shear zone was divided into three layers: deformation layers 1 and 2, and thermal conduction layer 0; each being of thickness δ. The following constitutive equation was used:

$$F_i(\tau_i, T_i) = \frac{\dot\gamma_i(t)}{\dot\varepsilon_\Phi} = \frac{T_i + 1}{C + 1} \exp \frac{\tau_i - 1 + a(T_i - C)}{b(T_i + 1)} \quad (i = 1, 2) \tag{1}$$

in this model [44]. Here $\dot\gamma(t)$ denotes the deformation velocity in the shear zone at time t, $\dot\varepsilon_\Phi$ is the mean deformation velocity in the case of continuous chips, while T_i and τ_i denote the temperatures and plastic shear stresses in the layers. This Arrhenius-type equation describes the effect of thermal softening and deformation velocity on the shear stress, in the shear zone of the workpiece. Here we used the so-called velocity-modified temperature $T_m = T(1 - k\log(\dot\gamma T_\Phi) + k\log(\varepsilon_\Phi T))$ that was introduced by MacGregor and Fisher [45]. The coefficient k is a constant characteristic of the material, which is—according to their measurements—$k = 0.008 - 0.045$. The thermal softening is characterized by the constant $\nu = -\Delta\tau/\Delta T_m$. In Eq. (1), $a = \nu T_w/\tau_\Phi$, where T_w is the absolute temperature of the workpiece, τ_Φ is the mean shear stress [7] in the shear zone during the formation of continuous chips, and $b = ka$. C denotes the absolute temperature T_Φ of the shear zone during the formation of continuous chips.

The derivation of the aforementioned model can be summarized as follows: the plastic shear stress τ_i $(i = 1, 2)$ occurring in the shear zone of size h_1 is in mechanical balance with the normal stress σ acting on length L (see Fig. 2). Thus, $\sigma L = \tau_2 h_1$. The normal stress σ causes an elastic deformation Δu in the chip, parallel with the u direction. Thus, $\sigma = E\Delta u/h_1$, i.e., $\dot\sigma = (E/h)\dot u \sin\Phi$. Here E denotes the Young modulus. The relative velocity can be calculated as $\dot u = v_{\Phi,\mathrm{Tool}} - v_{u,\mathrm{Material}} = v\cos\Phi - \delta\dot\gamma$. Since the velocity of plastic shear deformation is $\dot\gamma = v/\delta$, the consideration of two deformation layers—denoted by 1 and 2 in Fig. 2—implies $\dot u = \delta\dot\varepsilon_\Phi(1 - \dot\gamma_1/\dot\varepsilon_\Phi - \dot\gamma_2/\dot\varepsilon_\Phi)$. According to the mechanical balance,

$$\dot\tau_2 = \frac{ELv}{h^2}\sin^2\Phi\cos\Phi\left(1 - \frac{\dot\gamma_1}{\dot\varepsilon_\Phi} - \frac{\dot\gamma_2}{\dot\varepsilon_\Phi}\right). \tag{2}$$

For the sake of simplicity, we introduced a nondimensional time $\hat t = t/K$ and nondimensional shear stress $\hat\tau_i = \tau_i/\tau_\Phi$. According to the generally accepted approximation of the cutting theory, this latter quantity can be considered as a material constant. Using the new time scale and the notation

$$F_i = \frac{\dot\gamma_i}{\dot\varepsilon_\Phi}, \tag{3}$$

the equation of mechanical balance leads to the differential equation

$$\dot\tau_2 = 1 - (F_1 + F_2). \tag{4}$$

We found that

$$\tau_1 = p\tau_2 + s \tag{5}$$

$$\text{if} \quad K = \frac{\tau_\Phi h^2}{EL\nu \sin^2 \Phi \cos \Phi} \quad \text{and} \tag{6}$$

$$p = 1 + (\sqrt{3}\delta/h)\sin \Phi, \tag{7}$$

where the constant s depends on the initial conditions.

Besides the deformation bands 1 and 2, we introduced a 'quasi' layer (denoted by 0 in Fig. 2), too, where no plastic deformation occurs, but this layer plays an important role in the thermal processes. The variation of the material's heat content ($c\rho\dot{T}$, where c means heat capacity and ρ is density) during chip formation is composed of three elements, as was shown in [46]:

- mechanical power $r\tau_i\dot{\gamma}_i$, $(i = 1, 2)$, where r is energy ratio ($r \approx 0.95$),
- thermal conduction only occurring on the boundary surfaces of the layers; here we can use the simplified form of the differential equation of thermal conduction $4\lambda(T_i - T_{i-1})/\delta^2$ $(i = 0, 1, 2)$, where in the quasi-layer $(i = 0)$, $T_{i-1} = T_w$,
- the material progressing in direction w (Fig. 2) with velocity $v_c = v\sin(\Phi)$ conducts heat itself, which is $c\rho(T_i - T_w)/v_c$ $(i = 0, 1, 2)$.

Using these components, and introducing the dimensionless temperature $\hat{T}_i = (T_i - T_w)/T_w$, we compiled the differential equations of temperature variation for the three layers 0,1 and 2. Consequently, the energy balance equations for these layers assume the following dimensionless forms (here we already discarded the hat symbol):

$$\dot{T}_0 = \zeta(T_1 - 2T_0) - \xi T_0, \tag{8}$$

$$\dot{T}_1 = \eta\tau_1 F_1(\tau_1, T_1) - \zeta(2T_1 - T_2 - T_0) - \xi(T_1 - T_0), \tag{9}$$

$$\dot{T}_2 = \eta\tau_2 F_2(\tau_2, T_2) - (\xi + \zeta)(T_2 - T_1) \tag{10}$$

with the system parameters

$$\eta = \frac{rK\nu\tau_\Phi \cos \Phi}{c\rho\delta T_w}, \quad \xi = \frac{K\nu \sin \Phi}{\delta}, \quad \zeta = \frac{4K\lambda}{c\rho\delta^2}, \tag{11}$$

where λ denotes the thermal conductivity. Parameters p, ξ, and η characterize the geometry, the mechanical conditions, and the intensity of energy conduction, respectively. All of these three parameters are independent of the cutting speed v, since the expressions of ξ and η contain the Kv product. The expression of parameter ζ contains two time scales: the mechanical time scale K and the thermal time scale $\lambda/(c\rho)$. The behaviour of the system strongly depends on the relation of these scales. As we will show later, the mathematical model may lead to fundamentally different solutions at different values of ζ, as has also been experienced in practice.

Thus, the mathematical model of chip formation consists of the autonomous differential equations (4) and (8)–(10), together with the constitutive equation (1). The parameters are given by Eqs. (6), (7), and (11). The usual initial conditions are $\tau_2(0) = 1$ and $T_i(0) = 0$ ($i = 0$, 1, and 2), which leads to $s = 1 - p$.

3. Expansion of the 4D model to varying cutting speed

The cutting speed may vary during machining. The most obvious example for such processes is flat turning, but taper-turning, so-called 'back turning' and special polygon-turning also lead to variations in the cutting speed, which can be expressed as $v = v_0 f(t)$, where v_0 is a reference value. In nondimensional form, we obtain

$$\hat{v} = v/v_0 = f(t) = f(K\hat{t}). \tag{12}$$

Substituting $v = v_0 f(t)$ into Eq. (2), we arrive at the new form of Eq. (4):

$$\dot{\tau}_2 = f(1 - (F_1 + F_2)). \tag{13}$$

Expression (6) of the time scale K does not change with the substitution $v = v_0$. Since the expressions of the system parameters η and ξ contain the velocity v, the substitution $v = v_0 f$ is also necessary here. Thus, the energy balance equations also change to the following:

$$\dot{T}_0 = \zeta(T_1 - 2T_0) - f\xi T_0, \tag{14}$$

$$\dot{T}_1 = f\eta\tau_1 F_1(\tau_1, T_1) - \zeta(2T_1 - T_2 - T_0) - f\xi(T_1 - T_0), \tag{15}$$

$$\dot{T}_2 = f\eta\tau_2 F_2(\tau_2, T_2) - (f\xi + \zeta)(T_2 - T_1). \tag{16}$$

Thus, in the case of varying cutting speed, the mathematical model of chip formation consists of the constitutive equations (1), together with the differential equations (13)–(16). The constants, the system parameters and the initial conditions

remain unchanged. We complement this system in the following sections with the differential equation describing the oscillations of the workpiece. The extended model—which is analysed in this paper from the point of view of the design of technology—describes the periodic and aperiodic behaviour of the machine-tool-workpiece system.

4. The elastic, vibrating system

The machine-tool-workpiece system performs elastic vibrations as the cutting force varies. The natural frequencies of the cutting machine are usually higher than that of the tool or the workpiece. Thus, the elasticity of the machine has no significant effect on the dynamics and can be neglected. In the following we assume that one end of the beam-shaped workpiece is fixed in the chuck of the turning machine.

The velocity of the motion related to the oscillation of the workpiece and/or the tool is added to the cutting velocity. Thus, the resulting cutting velocity cannot be considered as constant, even in the case of simple turning with a constant revolution number n. This variation affects the chip formation. The workpiece is modelled as a beam with one end fixed, and the principal cutting force is applied at the other end of the beam. The oscillation of this 1DoF system can be described by the well-known differential equation

$$m_r\ddot{z} + \frac{z}{k} = F_v, \tag{17}$$

where m_r denotes the equivalent mass of the workpiece or tool, reduced at the point of action of the force, and k (m/N) is the spring constant. The principal cutting force F_v can be approximated as

$$F_v \approx c_F \tau_\Phi \quad \text{where}$$

$$c_F \approx (\operatorname{cotan}\Phi + \operatorname{cotan}\rho_\Phi)q. \tag{18}$$

τ denotes the shear stress in the shear zone in plastic state, while q denotes the area of the cross section of the cut layer [47]. ρ_Φ is the angle of 'internal friction', which can be defined in the shear zone, and can be expressed by the angle of friction $\bar{\rho}$ between the workpiece and the tool. Usually $\rho_\Phi = \pi/2 - (\Phi - \alpha + \bar{\rho})$, while in our case $\rho_\Phi = \pi/2 - \bar{\rho}$, i.e., $\operatorname{cotan}\rho_\Phi = \tan\bar{\rho} = \mu$, where μ denotes the usual Coulomb coefficient of friction. $c_F \approx 2$ if the area of the cross section of the cut layer is $q = 0.73\,\text{mm}^2$, the corresponding angles are $\Phi = 30^\circ$ and $\rho_\Phi = 45^\circ$, and τ_Φ is measured in MPa.

Characteristic of such technological problems, the point of action of the force usually approaches (or rarely, moves away from) the fixed end of the workpiece during turning. Consequently, the spring constant k decreases, and may assume a rather small value during the final part of the process. This variation is slow, and we assume in our model that $k = \text{const}$. To rewrite the equations in a dimensionless form, we introduce the notation

$$z = L'\hat{z}, \tag{19}$$

where the appropriate choice of L' is

$$L' = \frac{2\tau_\Phi}{m_r}K^2. \tag{20}$$

Discarding the special symbols showing the dimensionless nature of the quantities, we obtain

$$\ddot{z} + Az = \tau, \tag{21}$$

where

$$A = \frac{K^2}{km_r}. \tag{22}$$

According to what we have mentioned above, the final value of A may be several times larger than its initial value. The equivalent mass m_r of the beam is approximately $m_r \approx m/3$ for the workpiece fixed at one end.

The period of the free oscillations of the beam can be obtained as

$$T_{\text{per}} = \frac{2\pi}{\sqrt{A}} = 2\pi\frac{\sqrt{m_r k}}{K}, \tag{23}$$

while the angular natural frequency is

$$\omega = \frac{\sqrt{A}}{K}. \tag{24}$$

We can estimate the order of magnitude of A, based on a cutting experiment [48]. The angular frequency was $\omega = 2\pi \cdot 1800\,\text{rad/s}$, which corresponds to $T_{\text{per}} = 1/1800 = 5.56 \times 10^{-4}\,\text{s}$.

Consequently, $\sqrt{A} = 1800 \cdot 2\pi K = 1.1304 \times 10^4 K$, for example at $K = 1.769 \times 10^{-4}$, we obtain $A = 4$. The velocity of the workpiece, related to the oscillation is denoted by $\dot{z}$. According to Fig. 3, this velocity must be subtracted from the circumferential velocity v—i.e., from the nominal cutting speed—to obtain the effective cutting speed v_{ef}. In the extremal case, when $\dot{z}$ is equal to the circumferential velocity, no chip is produced.

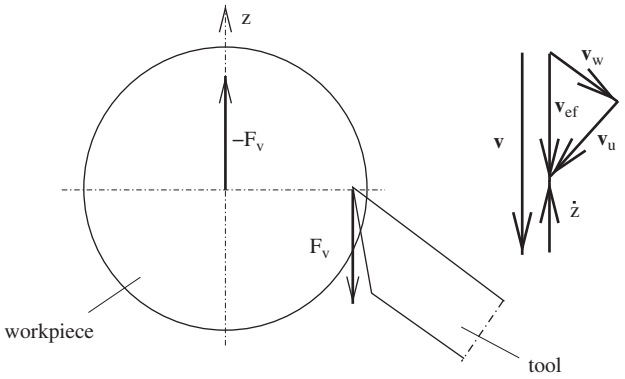

Fig. 3. Relations among the velocity components in the elastic workpiece-tool system.

The function f, that expresses the variation of velocity, can be given in dimensionless form as follows:

$$f = 1 - \frac{\dot{z}}{v_0}\frac{L'}{K} = 1 - \frac{\dot{z}}{V_0}, \tag{25}$$

where the dimensionless form of the reference (nominal) cutting speed v_0 is

$$V_0 = \hat{v}_0 = \frac{Kv_0}{L'} = \frac{m_r v_0}{2\tau_\Phi K}. \tag{26}$$

Consequently, A and V_0 are related to each other:

$$AV_0 = \frac{Kv_0}{2\tau_\Phi k}. \tag{27}$$

5. Model of chip formation as an oscillator during the turning process

The two models are combined if we substitute Eq. (25)—using Eq. (5)—into Eqs. (13)–(16), and consider that the stress τ in Eq. (21) is equivalent to the stress τ_2 introduced in the 4D model of chip formation. The resulting set of equations is the following at speeds $v_i = f_i v_0$:

$$\dot{\tau}_2 = f_i\left(1 - \frac{\dot{z}}{V_0}\right)(1 - (F_1 + F_2)), \tag{28}$$

$$\dot{T}_0 = \zeta(T_1 - 2T_0) - f_i\left(1 - \frac{\dot{z}}{V_0}\right)\xi T_0, \tag{29}$$

$$\dot{T}_1 = f_i\left(1 - \frac{\dot{z}}{V_0}\right)(\eta(\tau_2 p + 1 - p)F_1(\tau_1, T_1) - \xi(T_1 - T_0)) - \zeta(2T_1 - T_2 - T_0), \tag{30}$$

$$\dot{T}_2 = \eta f_i\left(1 - \frac{\dot{z}}{V_0}\right)\tau_2 F_2(\tau_2, T_2) - \left(f_i\left(1 - \frac{\dot{z}}{V_0}\right)\xi + \zeta\right)(T_2 - T_1), \tag{31}$$

$$\ddot{z} = \tau_2 - Az. \tag{32}$$

If the deformation of the tool was modelled instead of the deformation of the workpiece, the same equations could be used, with the z-axis reversed.

6. Discussion. Application for the oscillations of a typical workpiece

It can be checked using the cutting examples described in [9,10] that the vibrations of the elastic machining system have a considerable influence on the process. This fact has been demonstrated—among several other experiences—by [48]. Here we would like to show that our expanded model describes this phenomenon, indeed. Three realistic technological examples are considered, which are related to our earlier examples [9,10]. The system parameters of the 4D model were $a = 0.3$, $b = 0.012$, $C = 1$, $p = 1.03$, and—at the cutting speed $v_1 \equiv v_0 = 3.6\,\mathrm{m/s}$ ($f_1 = 1$), leading to periodic solutions—$\xi = 4.8$, $\eta = 4.4$, and $\zeta = 3.4$. The time scale was $K = 1.64 \times 10^{-4}\,\mathrm{s}$. We also examined the system at two

additional cutting speeds. At $v_2 = 0.58\,\mathrm{m/s}$ ($f_2 = 0.58/3.6 = 0.16$) we obtained chaotic solutions, while at $v_3 = 0.3\,\mathrm{m/s}$ ($f_3 = 0.3/3.6 = 0.083$) we obtained fixed point solutions.

Let the turned workpiece be a beam of size $\varnothing 40 \times 200\,\mathrm{mm}$, with $\tau_\Phi = 900\,\mathrm{MPa}$. The equivalent mass of this beam is approximately $m_r \approx 0.662\,\mathrm{kg}$, with spring constant $k = 1.0616 \times 10^{-7}\,\mathrm{m/N}$, and eigenfrequency $\nu \approx 600\,\mathrm{Hz}$. Using these values, the nondimensional constant A and velocity V_0 in Eq. (21) can be expressed; according to (20), (22), and (26), $L' = 0.0732$, $A = 0.383$, and $V_0 = 8.07$.

6.1. Modification of the stable periodic solution of the original 4D model

The solution of the oscillator model, described in Section 4, can be seen in Figs. 4 and 5, at cutting speed $v_1 = 3.6\,\mathrm{m/s}$. The so-called principal cutting force—which is parallel with the cutting speed—can be obtained using (18): $F_\nu = 2\tau_\Phi = 1800\,\mathrm{N}$. The static deflection of the beam is $z_{\mathrm{stat}} = F_\nu k \approx 1.9 \times 10^{-4}\,\mathrm{m} = 0.19\,\mathrm{mm}$ under this force. As it can be seen in Fig. 4a, the initial amplitude of the evolving oscillations is $\hat{z} \approx 2.2$. The real value of this amplitude is $z = L'\hat{z} = 0.16\,\mathrm{mm}$. This value is a little less than the static deflection. As it is clearly visible, the amplitude increases initially, but the motion becomes stationary at about $t = 2000$ (Figs. 4b and 5a).

According to Fig. 5a, the amplitude is approximately $\hat{z} \approx 21$ in this state, which corresponds to very large deflections of 1.5 mm. Thus, the originally periodic process of chip formation may lead to harmful oscillations in the case of certain workpieces with critical geometry. This fact is well known in engineering practice, so this result provides evidence of the applicability of our model. The eigenfrequency $\nu \approx 600\,\mathrm{Hz}$ of the workpiece and its harmonics at $\nu \approx 600k\,\mathrm{Hz}$ ($k = 1, 2, \ldots$) are clearly visible in the power spectrum of the oscillations (Fig. 5b), together with another large peak at about 14 000 Hz. Thus, the motion became quasiperiodic as the oscillations of the workpiece and the chip formation process superimposed. Note that if the two subsystems are not combined but the numerical simulations are performed independently with $\tau_2(0) = 1$, the amplitudes remain constant with $z = 2.7$ that corresponds to 0.19 mm.

6.2. Modification of the aperiodic (chaotic) solution of the original 4D model

At the cutting speed $v_2 = 0.58\,\mathrm{m/s}$, the solution of the original 4D model was chaotic, with Lyapunov exponent $\lambda \approx 634\,1/\mathrm{s}$ [10]. We also experienced chaotic behaviour during the initial part of the numerical simulation in the expanded

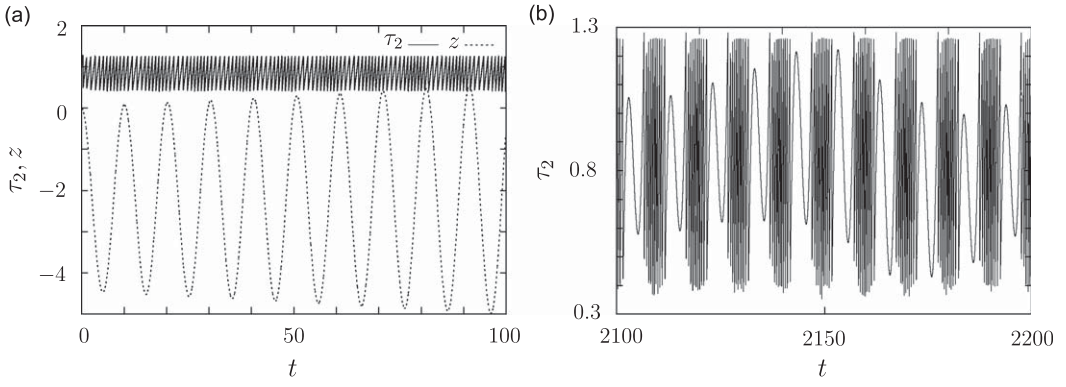

Fig. 4. Simulation results at $v_1 = 3.6\,\mathrm{m/s}$: (a) increasing amplitudes, (b) stationary oscillation of τ_2.

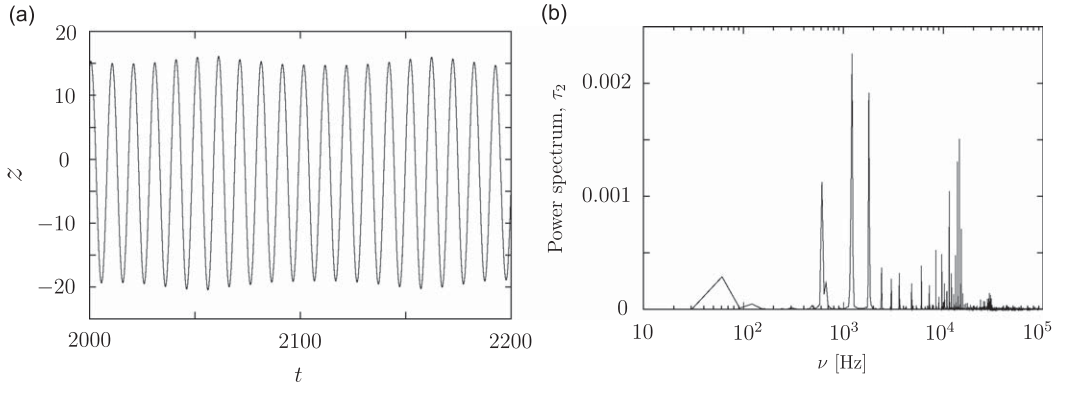

Fig. 5. Quasiperiodic oscillations at $v_1 = 3.6\,\mathrm{m/s}$: (a) stationary oscillation of z, (b) power spectrum.

system, at $f_2 = 0.16$ (Fig. 6a). There is still a peak in the spectrum at $\nu \approx 600$ Hz, but this is not dominant, and there are many more frequencies in the spectrum than in the previous case (Fig. 6b). To characterize the chaotic behaviour, we analysed the time series obtained by numerical simulation. First, we detected the maxima of τ_2 and plotted each value against the previous value (Fig. 7a). The geometric structure that can be seen in the figure is the projection of the chaotic attractor. Since the phase-space is six-dimensional with the variables τ_2, T_0, T_1, T_2, z, and $\dot{z}$, it cannot be plotted in full detail. However—according to Taken's embedding theorem [49]—if m delayed values of a single variable of a time series are considered, we obtain another m dimensional space, where the image of the chaotic attractor will be topologically similar to its original image in the real 6D phase-space. This is why the structure shown in Fig. 7a is actually a 2D projection of the attractor. The position vectors in this reconstructed phase-space assume this form:

$$\mathbf{r}_n = (\tau^{\max}_{n-(m-1)}, \tau^{\max}_{n-(m-2)}, \ldots, \tau^{\max}_{n-1}, \tau^{\max}_{n}). \tag{33}$$

Our primary goal is to show that the types of the solutions may change if the vibrations of the workpiece are included into the model. Thus, from this point of view not the exact values of the Lyapunov exponents are important; we are searching for evidence for the exponential divergence of trajectories. One of the most frequently used algorithms for the estimation of the Lyapunov exponents is Wolf's method [50]. Unfortunately, this algorithm and its modified versions do not allow one to test for the presence of exponential divergence, but just assume its existence. This is why we used the TISEAN software package, designed for nonlinear time series analysis [51,52], to examine the divergence of nearby trajectories, based on the time series of the maxima of τ_2.

The algorithm used for the calculation of the maximal Lyapunov exponent is the following: one chooses a point $\mathbf{r}_{n_0}$ in the m dimensional embedding space and selects all neighbours with a distance smaller than ε. The distance of these points will increase as the function of the relative time $\Delta n = n - n_0$. Repeating this process for N values of n_0, one obtains the average rate of expansion:

$$S(\varepsilon, m, \Delta n) = \frac{1}{N}\sum_{n_0=1}^{N} \log\left(\frac{1}{|\mathscr{U}(\mathbf{r}_{n_0})|}\sum_{\mathbf{r}_n \in \mathscr{U}(\mathbf{r}_{n_0})} |\tau^{\max}_{n_0+\Delta n} - \tau^{\max}_{n+\Delta n}|\right). \tag{34}$$

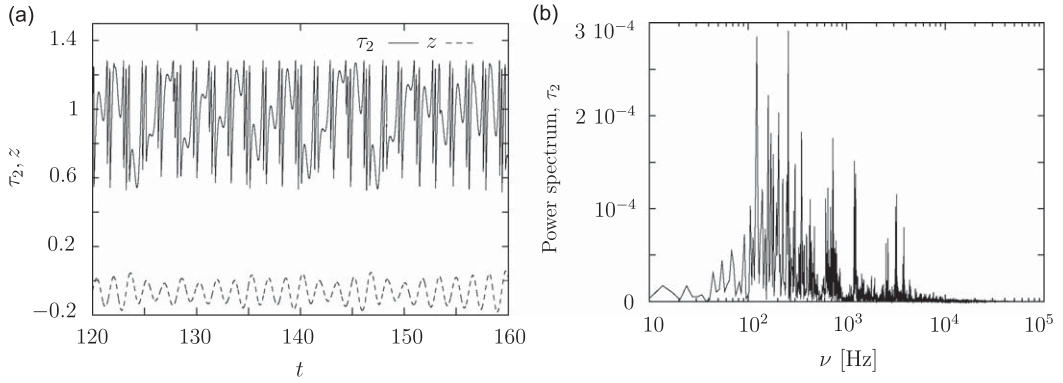

Fig. 6. Chaotic oscillations at $v_2 = 0.58$ m/s: (a) time series of τ_2 and z, (b) power spectrum.

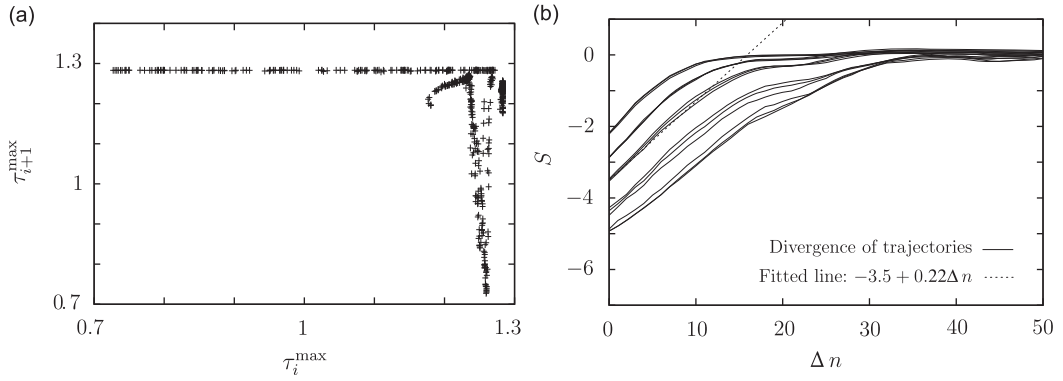

Fig. 7. Time series analysis of the chaotic part of the signal at $v_2 = 0.58$ m/s: (a) a projection of the attractor, (b) estimation of the Lyapunov exponent.

Here, $\mathscr{U}(\mathbf{r}_{n_0})$ is the neighbourhood of the delay vector $\mathbf{r}_{n_0}$ with diameter ε. If $S(\varepsilon, m, \Delta n)$ exhibits a linear increase with a certain slope, this slope can be taken as an estimate of the maximal Lyapunov exponent λ (Fig. 7b).

Naturally, two trajectories cannot separate further than the size of the attractor, which is why a saturation can be observed in Fig. 7b. Averaging the estimated slopes of the linear parts of the curves, we were able to fit a line with slope $\hat{\lambda} \approx 0.22$. This slope is the nondimensional approximation of the Lyapunov exponent. Taking into account that the time step was 0.0005 during the simulation, there were on average 930 steps between two maxima of τ_2, and the time scale was $K/f_2 = 1.025 \times 10^{-3}$, the Lyapunov exponent can be approximated as $\lambda \approx 0.22/(0.0005 \cdot 930 \cdot K/f_2) = 462\,1/\mathrm{s}$. Since both the linear parts of the curves and the saturation are clearly visible in Fig. 7b, we can claim that the examined solution is chaotic during the first part of the simulation. However, later this chaotic state comes to an end, as Fig. 8a shows.

The eigenfrequency $\nu \approx 600\,\mathrm{Hz}$ is dominant in the spectrum if the first part of the time series ($t < 1000$) is discarded (see Fig. 8b), and there is another peak, too. Consequently, the chaotic motion—after a period of time the duration of which sensitively depends on the initial conditions—switches to quasiperiodic vibration. This phenomenon is referred to as transient chaos. Note that since parameter A increases during the process, we also examined the behaviour of the system at larger values of A. According to our experiences, the mean lifetime of transient chaos decreases as parameter A is increased. Moreover, at a sufficiently large value, the final solution becomes fixed point, instead of a quasiperiodic vibration.

6.3. Modification of the fixed point (equilibrium) solution of the original 4D model

At the cutting speed $v_3 = 0.3\,\mathrm{m/s}$, the solution of the original 4D model was a fixed point. However, we observed aperiodic vibrations in the extended model with $f_3 = 0.083$. The deflection-time diagram can be seen in Fig. 9.

To determine the characteristics of the motion, we again applied nonlinear time series analysis. Plotting the subsequent values of the maxima of the shear stress τ_2, we obtained Fig. 10a, where the points form a geometric structure. The analysis of the time series composed of these values led to Fig. 10b. The slope of the linear part of the curves provides a nondimensional estimation for the Lyapunov exponent, which is approximately $\hat{\lambda} \approx 0.17$. Since the time step was 0.0005 during the simulation, the average number of steps between two minima was 507.4 and the time step is $K/f_3 = 1.97 \times 10^{-3}\,\mathrm{s}$, the real value of the Lyapunov exponent is $\lambda \approx 0.17/(0.0005 \cdot 507 \cdot K/f_3) = 340\,1/\mathrm{s}$.

This result is verified by the section of a continuous chip, shown in Fig. 11, where $z_{\mathrm{ampl}} \approx 0.015\,\mathrm{mm}$. It is usual in practice, that an irregular (chaotic), small amplitude unevenness occurs on the profile of continuous chips (fixed point

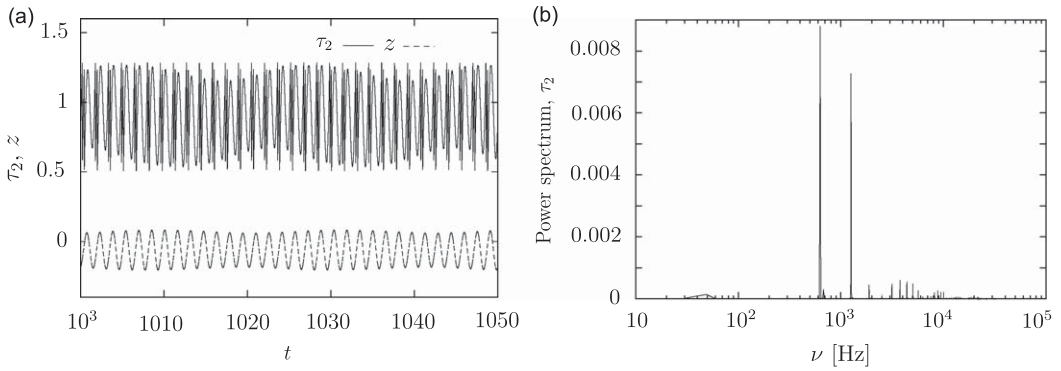

Fig. 8. Quasiperiodic vibrations after the chaotic part of the motion, at $v_2 = 0.58\,\mathrm{m/s}$: (a) τ_2 and z, (b) power spectrum.

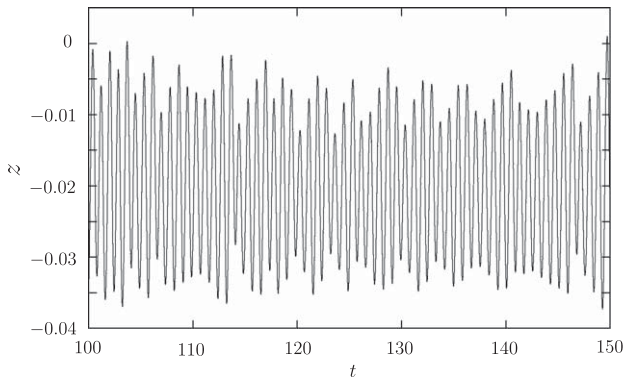

Fig. 9. Deflection-time diagram at $v_3 = 0.3\,\mathrm{m/s}$.

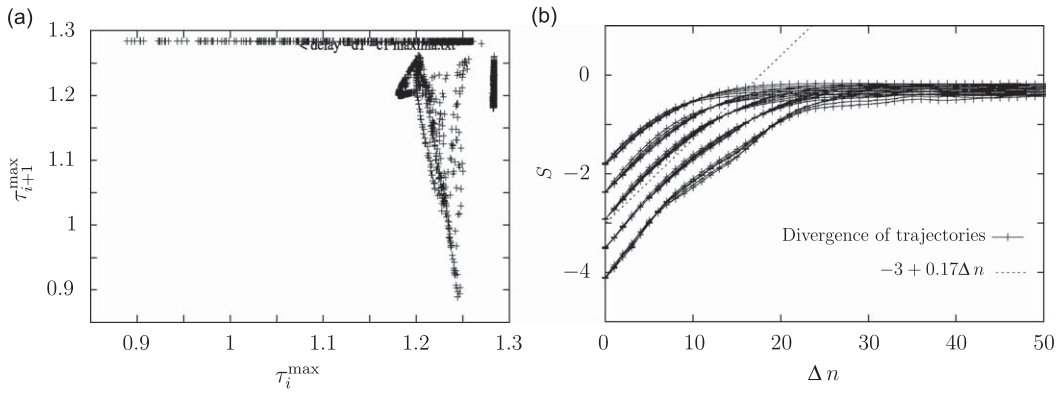

Fig. 10. Time series analysis of the chaotic part of the signal at $v_3 = 0.3\,\mathrm{m/s}$: (a) a projection of the attractor, (b) estimation of the Lyapunov exponent.

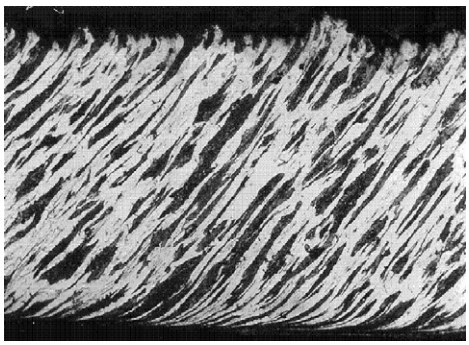

Fig. 11. Continuous chip with chaotic unevenness.

solutions). This phenomenon refers to the small oscillations of the machine-tool-workpiece system, according to the results of our cutting model. The calculated value, $z \approx 0.014\,\mathrm{mm}$, is consistent with the measured amplitude on the chip section.

7. Conclusion

We can conclude that the assumption about the elasticity of the workpiece led to a significantly more complex mathematical model, and—in the examined typical cases—more complex types of solutions. Compared to the 4D model, the analysis of the time series was rather difficult in the 6D model, and the precision of the estimations decreased. The types of evolving solutions also changed:

- Due to the interaction between the oscillating workpiece and the formation of chips, the originally periodic cutting process became quasiperiodic. The eigenfrequency of the workpiece appeared in the spectrum of the vibration.
- The originally chaotic solution of the 4D model became transient chaotic. The Lyapunov exponent is less during the chaotic part of the motion than it was in the 4D model. After a sufficiently long time, the motion suddenly becomes quasiperiodic.
- In the case of the original equilibrium (fixed point) solution, we found small amplitude chaotic vibrations. This result is in agreement with the practical experience, i.e., that the chip width varies slightly and irregularly in the case of continuous chips, too.

We believe that this simple model makes a quick overview of the sources of vibrations during the cutting process possible. Moreover, it can provide help during the design and evaluation of preliminary experiments and measurements that are necessary for the preparation of the production process. In the case of large simulation software, our model may support the design or can be used for the determination of certain parameters in applications.

Acknowledgements

This research project was supported by the Hungarian National Science Foundation under Grant no. OTKA F049242, and by the János Bolyai Research Scholarship of the Hungarian Academy of Sciences. The authors thank Dr. János Kodácsy (Kecskemét College, Faculty of Technology (GAMF)) for his help with the experimental examination of the nonlinear dynamics of the cutting process.

References

[1] S.A. Tobias, *Machine Tool Vibration*, Blackie and Son Ltd., Glasgow, 1965.
[2] E.J.A. Armarego, R.H. Brown, *The Machining of Metals*, Prentice-Hall, Inc., Englewood Cliffs, NJ, 1969.
[3] J. Tlusty, Analysis of the state of research in cutting dynamics, *CIRP Annals* 27 (1978) 583–589.
[4] S. Doi, Chatter of lathe tool, *Journal of Society of Mechanical Engineers, Japan* 3 (1937) 94.
[5] H. Ernst, M. Martellotti, The formation of the built-up edge, *ASME Mechanical Engineering* 57 (1938) 478–498.
[6] J.S. Shteinberg, *Elimination of Vibrations Excited During Turning*, Mashgiz, Moscow, 1947 (in Russian).
[7] V. Piispanen, Theory of chip formation, *Teknillinen Aika Kauslehti* 27 (1937) 315 (in Finnish).
[8] P. Landberg, Vibrations caused by chip formation, *Microtechnic* 10 (1956) 219.
[9] P. Albrecht, Self-induced vibrations in metal cutting, *Transactions of the American Society of Mechanical Engineers Series B Journal of Engineering for Industry* 84 (1962) 405.
[10] R. Komanduri, T. Schroeder, J. Hazra, B.F. von Turkovich, On the catastrophic shear instability in high-speed machining of an AISI 4340 steel, *Journal of Engineering Industry* 104 (1982) 121–131.
[11] R. Komanduri, Machining and grinding: historical review of the classical papers, *Applied Mechanics Reviews* 46 (1993) 80–132.
[12] M. Field, M.E. Merchant, Mechanics of formation of discontinuous chip in metal cutting, *Transactions of the American Society of Mechanical Engineers* 71 (1949) 421.
[13] R.F. Recht, Catastrophic thermoplastic shear, *ASME Journal of Applied Mechanics* 31 (1964) 189–193.
[14] M.C. Shaw, Assessment of machinability, ISI Special Report 94, Vol. 1, Iron and Steel Institute, London, 1967.
[15] R. Komanduri, Z.-B. Hou, On thermoplastic shear instability in the machining of a titanium alloy (Ti–6Al–V), *Metallurgical and Materials Transactions* 33A (2002) 2995–3010.
[16] M. Shi, S.A. Tobias, Theory of finite amplitude machine tool instability, *International Journal of Machine Tool Design and Research* 24 (1984) 45–69.
[17] G. Stépán, Delay-differential equation models for machine tool chatter, in: F.C. Moon (Ed.), *Dynamics and Chaos in Manufacturing Processes*, Wiley-Interscience Publication, New York, 1998, pp. 165–191.
[18] G. Stépán, Unstable quasiperiodic oscillations on machine tools, *Proceedings of GÉPÉSZET 2000*, Budapest, 2000, pp. 612–616.
[19] J. Gradisek, E. Govecar, I. Grabec, Using coarse-grained entropy rate to detect chatter in cutting, *Journal of Sound and Vibration* 214 (5) (1998) 941–952.
[20] J. Gradisek, E. Govekar, I. Grabec, Chatter onset in non-regenerative cutting: a numerical study, *Journal of Sound and Vibration* 242 (5) (2001) 829–838.
[21] J. Gradisek, I. Grabec, S. Siegert, R. Friedrich, Stochastic dynamics of metal cutting: bifurcation phenomena in turning, *Mechanical Systems and Signal Processing* 16 (5) (2002) 831–840.
[22] M.A. Johnson, Nonlinear Differential Equations with Delay as Models for Vibrations in the Machining of Metals, PhD Thesis, Cornell University, Ithaca, 1966.
[23] S. Doi, S. Kato, Chatter vibration of lathe tools, *Transactions of the American Society of Mechanical Engineers* 78 (1956) 1127.
[24] P. Potocnik, I. Grabec, Nonlinear model predictive control of a cutting process, *Neurocomputing* 43 (2002) 107–126.
[25] R. Rusinek, E. Szabelski, J. Warminski, Influence of the workpiece profile on the self-excited vibrations in a metal turning process, in: G. Randons, R. Neugebauer (Eds.), *Nonlinear Dynamics of Production Systems*, Wiley-VCH Verlag GmbH & Co. KGaA, Weiheim, 2004, pp. 153–167.
[26] T. Kalmár-Nagy, F.C. Moon, Mode-coupled regenerative machine tool vibrations, in: G. Randons, R. Neugebauer (Eds.), *Nonlinear Dynamics of Production Systems*, Wiley-VCH Verlag GmbH & Co. KGaA, Weiheim, 2004, pp. 129–151.
[27] I. Minis, B.S. Berger, Modelling, analysis and characterization of machining dynamics, in: F.C. Moon (Ed.), *Dynamics and Chaos in Manufacturing Processes*, Wiley, New York, 1998, pp. 125–163.
[28] I. Grabec, Chaos generated by the cutting process, *Physics Letters A* 117 (1986) 384–386.
[29] J.S. Lin, C.I. Weng, A nonlinear dynamic model of cutting, *International Journal of Machine Tools and Manufacture* 30 (1990) 53–64.
[30] J.S. Lin, C.I. Weng, Nonlinear dynamics of the cutting process, *International Journal of Machine Tools Manufacture* 33 (1991) 645–657.
[31] B.S. Berger, M. Rokni, I. Minis, Complex dynamics in metal cutting, *Quarterly of Applied Mathematics* VI (4) (1993) 601–612.
[32] R.F. Gans, When is cutting chaotic?, *Journal of Sound and Vibration* 188 (1) (1995) 75–83.
[33] F.C. Moon, H. Abarbanel, Chaotic motions in normal cutting of metals, Cornell University, Sibley School of Mechanical and Aerospace Engineering Report, 1995.
[34] S.T. Bukkapatman, A. Lakhantakia, S.R.T. Kumara, Analysis of sensor signals shows turning on a lathe exhibits low-dimensional chaos, *Physical Review E* 52 (1995) 2375–2387.
[35] R. Rusinek, K. Szabelski, J. Warminski, Vibration analysis of two-dimensional model of metal turning process, *Materials Science Forum* 440–441 (2003) 521–524.
[36] B.S. Berger, I. Minis, Y.H. Chen, A. Chavali, M. Rokni, Attractor embedding in metal cutting, *Journal of Sound and Vibration* 18 (1995) 936–942.
[37] G. Litak, Chaotic vibrations in a regenerative cutting process, *Chaos, Solitons and Fractals* 13 (2002) 1531–1535.
[38] G. Litak, R. Rusinek, A. Teter, Nonlinear analysis of experimental time series of a straight turning process, *Meccanica* 39 (2004) 105–112.
[39] A.K. Sen, G. Litak, A. Syta, Cutting process dynamics by nonlinear time series and wavelet analysis, *Chaos* 17 (2007) 023133.
[40] X.S. Wang, J. Hu, J.B. Gao, Nonlinear dynamics of regenerative cutting processes—comparison of two models, *Chaos, Solitons and Fractals* 29 (2006) 1219–1228.
[41] T.J. Burns, M.A. Davies, On repeated adiabatic shear band formation during high-speed machining, *International Journal of Plasticity* 18 (2002) 487–506.
[42] Z. Pálmai, G. Csernák, Chaotic phenomena induced by fast plastic deformation of metals (in the case of cutting), *Proceeding of GÉPÉSZET 2006*, Budapest, 2006.
[43] G. Csernák, Z. Pálmai, Exploration of the chaotic phenomena induced by fast plastic deformation of metals, *International Journal of Advanced Manufacturing Technology* 40 (2009) 270–276.
[44] Z. Pálmai, Aperiodic deformation occurring as a result of thermoplastic instability of metals, *Materials Science Forum* 537–538 (2007) 541–548.
[45] C.W. MacGregor, J.C. Fisher, A velocity-modified temperature for the plastic flow of metals, *Journal of Applied Mechanics* A11–A16 (1946).
[46] Z. Pálmai, Chaotic phenomena induced by the fast plastic deformation of metals during cutting, *ASME Journal of Applied Mechanics* 73 (2006) 240–245.
[47] M.C. Shaw, *Metal Cutting Principles*, Oxford Science Publications, 1984, pp. 21–22.
[48] J. Kodácsi, Measurement of the cutting force, Faculty of Technology of the Kecskemét College, not published.

[49] F. Takens, *Detecting Strange Attractors in Turbulence*, *Lecture Notes in Mathematics*, Vol. 898, Springer, New York, 1981.
[50] A. Wolf, J. Swift, H. Swinney, J. Vastano, Determining Lyapunov exponents from a time series, *Physica D* 16 (1985) 285–317.
[51] R. Hegger, H. Kantz, T. Schreiber, Practical implementation of time series methods: the TISEAN package, *Chaos* 9 (1999) 413–435.
[52] H. Kantz, T. Schreiber, *Nonlinear Time Series Analysis*, *Cambridge Nonlinear Science Series*, Cambridge University Press, Cambridge, 1997.